Model Calibration and Optimization of a Protein Purification Process

by

Sadiq Al-Kaisy

Department of Chemical Engineering
Lund University

June 2015

Supervisors: **Anton Sellberg & Niklas Andersson**
Examiner: **Professor Bernt Nilsson**

Postal address	**Visiting address**	**Telephone**
P.O. Box 124	Getingevägen 60	+46 46-222 82 85
SE-221 00 Lund, Sweden		+46 46-222 00 00
Web address		**Telefax**
www.chemeng.lth.se		+46 46-222 45 26

Acknowledgement

First of all, I would like to thank Professor Bernt Nilsson for giving me the opportunity to do this thesis at the Department of Chemical Engineering. I would also like to thank him for his advice and for sharing his knowledge.

I would like to thank my supervisors Anton Sellberg and Niklas Andersson for always being supportive and for helping me throughout this thesis.

Finally, I would like to thank all the people at the Department of Chemical Engineering for providing a pleasant atmosphere.

Abstract

Four different chromatography models were calibrated to describe the separation of a ternary protein mixture consisting of lysozyme, cytochrome C and ribonuclease A in an ion-exchange chromatography column. The models are based on the same column model, the kinetic dispersive model. Protein adsorption was described by four different adsorption models, the Langmuir model with mobile phase modulators (MPM), the steric mass action (SMA) model, the self-association (SAS) model and the generalized Langmuir (GL) model. The models were calibrated against two kind of experiments, multi-component gradient experiments at low column load and single-component gradient experiments at high column load. The models were also validated against a multi-component validation experiment. All the models, especially the Langmuir MPM model, fit the experimental profiles at low column load very well. At high column load only the SAS model and GL model could capture the behavior of the experimental profiles, but even these two models did not fit the experimental profiles so well. The thesis was concluded with an optimization of the protein purification process. Three different objective functions were optimized, productivity, yield and normalized earnings. Optimization was performed with regard to two decision variables, the variables correspond to the amount of proteins loaded and the slope of the salt gradient, and one purity constraint. Maximum productivity was obtained at high column load and steep salt gradient. Maximum yield was obtained at low column load and flat salt gradient.

Table of Contents

1 Introduction

Chromatography is a separation technique that is widely used for both production and analytical purposes. In a chromatography process a mixture is introduced into a mobile phase. The mobile phase carries the mixture through a column that holds the stationary phase. Separation is achieved when the components in the mobile phase interact with the stationary phase. There are several chromatography techniques and these techniques utilize different characteristics of the components. For instance, in size-exclusion chromatography the components are separated due to the difference in the ability to penetrate the porous structure of the stationary phase. Since larger components penetrate less of the porous structure, they will encounter less volume than the smaller components and thus elute before the smaller components. In ion-exchange chromatography (IEC) charged components are separated due to the strength of interaction with the charged stationary phase [1].

Chromatography is commonly used in the biopharmaceutical industry. It is a technique that provides high yield and productivity while maintaining an acceptable product purity. The chromatography process in the biopharmaceutical industry usually constitutes most of the manufacturing cost [2]. Therefore it is important to optimize the chromatography process. Due to the complex behavior and the various parameters that are involved in a chromatography process, it is very difficult to optimize. One way to facilitate the optimization process is to use a mathematical-model that describes the chromatography process. A well-defined mathematical-model, that is consistent with experimental result, can not only be used to optimize the chromatography process but can also reduce the amount of experimental work that is generally performed in the developing of the chromatography process and therefore reduce costs [3].

1.1 Outline of this thesis

The main focus of this thesis is model-calibration of a protein purification process. Four different chromatography models were calibrated to describe the separation of a ternary protein mixture consisting of lysozyme, cytochrome C and ribonuclease A in an ion-exchange chromatography column. Several experiments were performed and used in the calibration of the different models. The work in this thesis was concluded with optimization of the protein purification process. In the optimization a calibrated and validated model was used.

2 Theory

2.1 Ion-exchange chromatography

In IEC the stationary phase is covered by charged ligands. Salt ions with opposite charge are adsorbed on the ligands. When a mixture is injected in the chromatography system, charged components will adsorb on the stationary phase and replace the salt ions. To desorb the charged components the salt concentration is increased in the mobile phase. The components will desorb according to their strength of interaction and thus separation is attained [1].

2.2 Models

The chromatography models that were used in the calibration are based on the same column model, the kinetic dispersive model. The kinetic dispersive model contains three parts dispersion, convection and adsorption [2]. The chromatography models differentiate in how the adsorption part is described.

2.2.1 Column model

The kinetic dispersive model lumps different phenomena together and expresses them as mainly three parts [2]. These phenomena are such as multi-path dispersion, axial diffusion, mass-transfer resistance between mobile phase and stationary phase and mass-transfer within the stationary phase. The column model for component *i* is described by the following equation [4]:

$$\frac{\partial c_i}{\partial t} = \underbrace{D_{ax}\frac{\partial^2 c_i}{\partial x^2}}_{Dispersion} - \underbrace{\frac{F}{\varepsilon A}\frac{\partial c_i}{\partial x}}_{Convection} - \underbrace{\frac{(1-\varepsilon_c)}{\varepsilon}\frac{\partial q_i}{\partial t}}_{Adsorption\ kinetic} \tag{2.1}$$

where c_i is the concentration of component *i* in the mobile phase, t is the time, D_{ax} is the axial dispersion coefficient, x is the length coordinate along the column, F is the volumetric flow, A is the column cross-sectional area, ε is the total porosity of the column, ε_c is the void fraction of the column and q_i is the concentration in the stationary phase. To solve equation (2.1) two boundary conditions had to be set. At the inlet of the column the concentration is assumed to be equal to the inlet concentration of the mobile phase, therefore a Dirichlet condition was set, see equation (2.2) [4].

$$c_i(t, 0) = c_{inlet,i} \tag{2.2}$$

At the outlet of the column only convective transport is considered therefore a Neumann condition was set, see equation (2.3) [4].

$$\frac{\partial c_i}{\partial x} = 0 \text{ at } x = L \tag{2.3}$$

L is the length of the column. As for initial values the column was assumed to be empty of proteins, see equations (2.4) and (2.5).

$$c_i(0, x) = 0 \text{ where } i = \{Lysozyme, Cytochrome\ C, Ribonuclease\ A\} \tag{2.4}$$

$$c_s(0, x) = c_{s,wash} \tag{2.5}$$

c_s is the salt concentration in the mobile phase and $c_{s,wash}$ is the salt concentration in the mobile phase that is used to wash the column.

2.2.2 Adsorption – Langmuir MPM model

In the Langmuir (MPM) model proteins compete with each other for the available ligands on the stationary phase whereas salt is considered to be an inert component [1]. The interaction between the proteins and the ligands is described as an equilibrium reaction, see equation (2.6).

$$c_i + q_{free,i} \underset{k_{des,i}}{\overset{k_{ads,i}}{\rightleftharpoons}} q_i \tag{2.6}$$

$k_{ads,i}$ is the adsorption coefficient, $k_{des,i}$ is the desorption coefficient and $q_{free,i}$ is the concentration of the available ligands. The effect of salt concentration on the protein interaction is described by a mobile phase modulator. Desorption coefficient is increased by a higher salt concentration in the mobile phase, see equation (2.7) [1].

$$k_{des,i} = k_{des0,i}\, c_s^{\beta_i} \tag{2.7}$$

β_i is a constant parameter that describes the ion-exchange characteristic and $k_{des0,i}$ is a modulator constant . The dynamic model of the adsorption can be seen in equation (2.8) [1].

$$\frac{\partial q_i}{\partial t} = k_{ads,i} c_i q_{max,i} \left(1 - \sum_{j=1}^{N} \frac{q_j}{q_{max,j}}\right) - k_{des,i} q_i \tag{2.8}$$

$q_{max,i}$ is the maximum concentration attainable in the stationary phase. Equation (2.8) can be rewritten as:

$$\frac{\partial q_i}{\partial t} = k_{des0,i}\, c_s^{\beta_i} \left(\frac{k_{ads,i} \cdot q_{max,i}}{k_{des0,i} \cdot c_s^{\beta i}} c_i \left(1 - \sum_{j=1}^{N} \frac{q_j}{q_{max,j}}\right) - q_i\right) =$$

$$= k_{kin,i} \left(B_i c_i c_s^{-\beta_i} \left(1 - \sum_{j=1}^{N} \frac{q_j}{q_{max,j}}\right) - q_i\right) \tag{2.9}$$

To simplify the calibration of the model, $k_{kin,i}$ was assumed to be independent of the salt concentration. This will result in that the $k_{kin,i}$ parameter can be used to adjust the width of the elution peaks while the B_i parameter can be used to adjust the retention time of the elution peaks [4].

2.2.3 Adsorption – The steric mass action model

In the SMA model proteins and salt ions compete with each other for the available ligands on the stationary phase. The interaction between the proteins and the ligands is described as an equilibrium reaction in which electro-neutrality must be conserved. When a protein adsorb on the stationary phase salt ions must desorb. Since proteins are large molecules and have several charges on the surface, adsorption occurs on more than one ligand. Adsorbed proteins also

shield a number of ligands, which become unavailable for other proteins, due to steric hindrance. The equilibrium reaction can be seen in equation (2.10) [1].

$$c_i + v_i\bar{q}_s \underset{k_{des,i}}{\overset{k_{ads,i}}{\rightleftharpoons}} q_i + v_i c_s \tag{2.10}$$

v_i is the number of ligands that a protein adsorb to and $\bar{q}_s$ is the concentration of available ligands. The maximum concentration attainable in the stationary phase can be expressed as following:

$$q_{max,i} = \frac{\Lambda}{v_i + \sigma_i} \tag{2.11}$$

Λ is the ligand density in the stationary phase and σ_i is the number of ligands shielded by the protein. The dynamic model of the adsorption can be seen in equation (2.12) [1].

$$\frac{\partial q_i}{\partial t} = k_{ads,i} c_i \left(\Lambda - \sum_{j=1}^{N} (v_i + \sigma_i)\, q_i\right)^{v_i} - k_{des,i} q_i c_s^{v_i} \tag{2.12}$$

This can be rewritten as:

$$\frac{\partial q_i}{\partial t} = k_{des,i}\left(c_i K_{eq,i}\left(\Lambda - \sum_{j=1}^{N} (v_i + \sigma_i)\, q_i\right)^{v_i} - q_i c_s^{v_i}\right) \tag{2.13}$$

$K_{eq,i}$ is the equilibrium constant of adsorption. Since salt also interact with the stationary phase it has to be modeled. The change of salt concentration on the stationary phase can be seen in equation (2.14) [1].

$$\frac{\partial q_s}{\partial t} = -\sum_{j=1}^{N} v_i \frac{\partial q_i}{\partial t} \tag{2.14}$$

2.2.4 Adsorption – The self-association model

The SAS model is similar to the SMA model. The adsorption of the proteins on the stationary phase is described the same way as in the SMA model. The difference is that in this model proteins can also dimerize. This means that proteins can adsorb on already adsorbed proteins of the same species. This will give rise to a different kind of isotherm, an isotherm that has anti-Langmuir behavior at low protein concentration and Langmuir behavior at higher protein concentration [5,6]. The dynamic model can be seen in equation (2.15) [5].

$$\frac{\partial q_i}{\partial t} = k_{des,i}\left(c_i K_{eq1,i}\left(\Lambda - \sum_{j=1}^{N} (v_i + \sigma_i)\, q_i\right)^{v_i} \cdot \left(1 + K_{eq2,i} c_i\right) - q_i c_s^{v_i}\right) \tag{2.15}$$

$K_{eq1,i}$ is the equilibrium constant of adsorption and $K_{eq2,i}$ is the equilibrium constant for the dimerization mechanism. The dynamic model is very similar to the SMA model, see equations (2.15) and (2.13).

2.2.5 Adsorption – The Generalized Langmuir model

The (GL) isotherm is defined in equation (2.16) [7].

$$q_i = \frac{H_i c_i}{1 + \sum_{j=1}^{N} (p_j K_j c_j)} \tag{2.16}$$

H_i is Henry's constant and K_j is the equilibrium constant of adsorption. p_j can assume the values ± 1, these values determine whether component j follows a Langmuir isotherm or an anti-Langmuir isotherm. If $p_j = 1$ the component follows the Langmuir isotherm and if $p_j = -1$ the component follows the anti-Langmuir isotherm. If one or more components follow the anti-Langmuir isotherm the model becomes limited. The limitation comes from the fact that the denominator in equation (2.16) should not have negative values, since that does not have any physical meaning. This means that not all compositions in the mobile phase are allowed [7]. Describing a component with an anti-Langmuir isotherm is also physically incorrect since there is an actual limit to how much a component can adsorb on the stationary phase. But even so the model can still be useful within limited operating conditions. The dynamic model with salt dependency included can be seen in equation (2.17).

$$\frac{\partial q_i}{\partial t} = k_{f,i}\left(\frac{H_i c_s^{-\beta_i} c_i}{1+\sum_{j=1}^{N}\left(p_j \frac{H_j c_s^{-\beta_j}}{q_{max,j}} c_j\right)} - q_i\right) \tag{2.17}$$

$k_{f,i}$ is a kinetic coefficient. The equilibrium constant of adsorption is rewritten in equation (2.17), $K_i = \frac{H_i}{q_{max,i}}$.

2.3 Isotherms

The adsorption models presented in this thesis follow different isotherms. The Langmuir MPM model and the SMA model follow a Langmuir isotherm. The SAS model follows an isotherm that has an anti-Langmuir behavior at low protein concentration and a Langmuir behavior at high protein concentration. The GL model can either follow the Langmuir isotherm or the anti-Langmuir isotherm depending on the sign of p_j parameter. Different isotherms will correspond to different concentration profiles for mass overloaded experiments i.e. different behavior of concentration profiles can be captured with different isotherms.

Linear isotherm, Langmuir-isotherm and anti-Langmuir isotherm and their corresponding concentration profiles for mass overloaded experiments can be seen in figure 1.

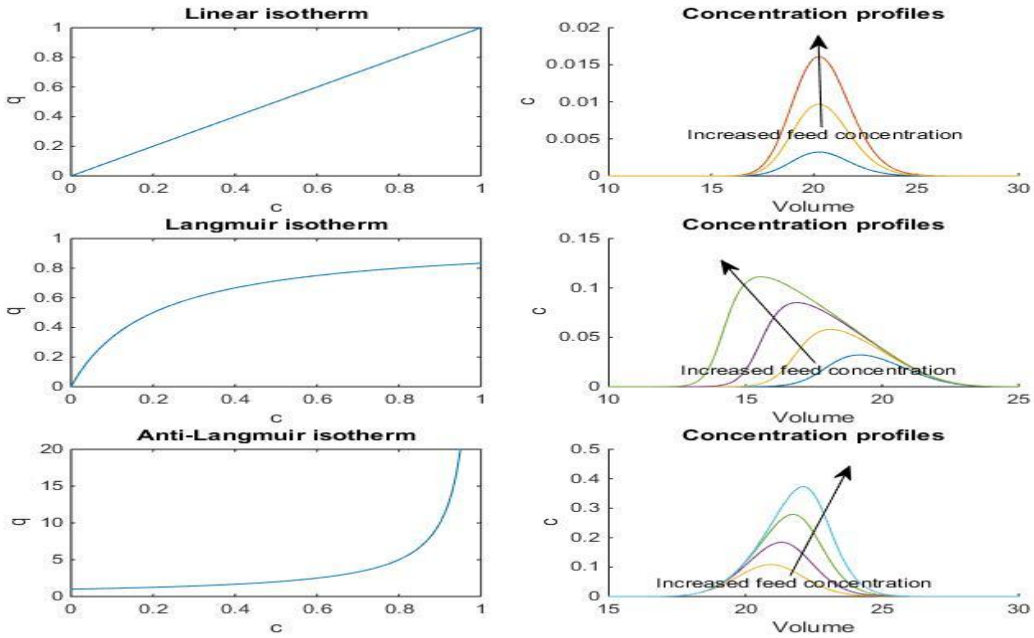

Figure 1. Different isotherms and their corresponding concentration profiles for mass overloaded experiments.

3 Chromatography system

A schematic description of the chromatography system used in this thesis can be seen in figure 2.

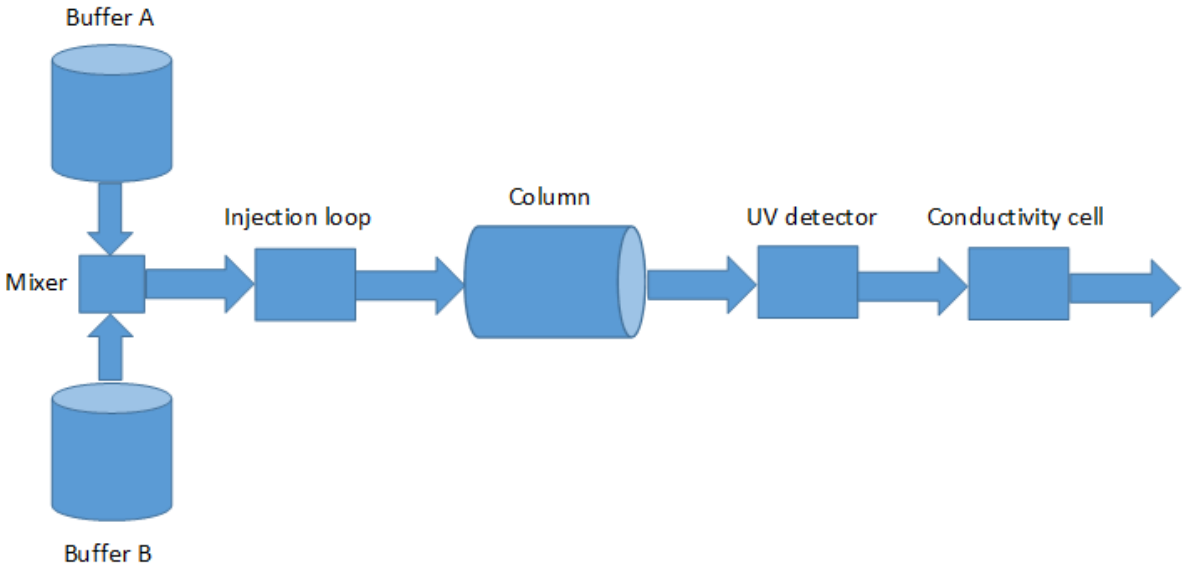

Figure 2. A schematic description of the chromatography system.

A chromatography experiment can be divided in basically four steps. The first step is to load the protein mixture onto the column. The protein mixture is introduced into the system through the injection loop. The second step is to wash the column. In this step a mobile phase with low salt concentration is used. The desired salt concentration is obtained by mixing Buffer A and Buffer B. Buffer A is a mobile phase with low salt concentration and Buffer B, the elution buffer, is a mobile phase with high salt concentration. The third step is to elute the proteins. Mobile phase with high salt concentration is pumped through the column. The final step is regeneration of the column. Pure Buffer B is pumped through the column to remove remaining proteins. The column is then washed, preparing it for a new load. The outlet of the column passes through a UV detector and a conductivity cell. Therefore an absorbance profile and a conductivity profile of the experiment are obtained.

4 Methods

Methods that were used and assumptions that were made to calibrate the parameters in the models are presented in this section. This section also include the simulation technique that was used to solve the column model and a description of the optimization process.

4.1 UV absorption coefficient

Calibration was performed by fitting the simulated profiles to the experimental profiles. Since experimental profiles were obtained from a UV detector they have absorbance unit. The profiles obtained from simulation are concentration profiles of the different proteins, therefore they have to be converted to a single absorbance profile before the calibration can be implemented. To convert the simulated concentration profiles to an absorbance profile two assumptions were made. The first assumption was that Beer's law is valid and the second assumption was that absorbance is an additive function, see equations (4.1) and (4.2) [8].

$$A_\lambda = \varepsilon_\lambda c l = Abs_\lambda c \tag{4.1}$$

$$A_{\lambda,Total} = \sum_{J=1}^{N} A_{\lambda,J} \tag{4.2}$$

A_λ is the absorbance at a specific wavelength λ, ε_λ is the absorptivity of the dissolved component, c is the concentration of the dissolved component, l is the light path length, Abs_λ is the absorption coefficient of the dissolved component, $A_{\lambda,Total}$ is the total absorbance and $A_{\lambda,J}$ is the absorbance of the dissolved component *J*.

The absorption coefficient of the different proteins were experimentally calculated. A single-component gradient elution experiment was performed for each protein. A small amount of the protein was loaded onto the column and then eluted with a salt gradient. Since the amount loaded onto the column is already known the absorption coefficient can be calculated using the derivation in equation (4.3). The experiments were repeated twice and a mean value was calculated.

$$A_\lambda = Abs_\lambda c \Longrightarrow \int A_\lambda(V)\ dV = Abs_\lambda \int c(V)\ dV \Longrightarrow Abs_\lambda = \frac{\int A_\lambda(V)\ dV}{\int c(V)\ dV} \tag{4.3}$$

V is the volume, $\int A_\lambda(V)\ dV$ is calculated from the experimental absorbance profile and $\int c(V)\ dV$ is the amount loaded onto the column. When the absorption coefficient of each protein was calculated, equations (4.1) and (4.2) were used to convert the concentration profiles of the different proteins to a single absorbance profile.

Wavelength of 280 nm was used for all experiments. This is because proteins absorb strongly at 280 nm while other components that are commonly in the protein solutions do not [8].

4.2 Conductivity and salt concentration

To estimate the salt concentration in the buffer solutions and the protein mixtures conductivity was measured. A linear relation between the conductivity and salt concentration was assumed,

see equation (4.4). The proportionality constant was calculated by measuring the conductivity of a solution with a known salt concentration [3].

$$c_s = A_{Con} Con \tag{4.4}$$

Con is the conductivity and A_{Con} is the proportionality constant.

4.3 Dead volume

Dead volume is the volume between the injection loop and the inlet of the column and the volume between the measure cells and the outlet of the column, see figure 2. The models in the theory section only simulate the column behavior while the experimental profiles include the dead volume, therefore the experimental profiles were modified before the calibration was implemented. The experimental profiles were moved to the left a volume equivalent to the dead volume to isolate the behavior of the column [1].

The dead volume was calculated with a tracer experiment [2]. An acetone solution was injected in the chromatography system while the column was replaced by a zero volume connector. Since acetone solution has higher absorptivity and lower conductivity than the mobile phase, a peak will appear in the absorbance profile and a dip in the conductivity profile, see figures 4 and 5. The profiles have a Gaussian appearance, therefore the volume at the peak and the volume at the vertex point of the dip can directly be used in the calculations of the dead volume, see equations (4.5) [2] and (4.6).

$$DV_{UV} = V_{peak} - V_{inj} - \frac{V_{loop}}{2} \tag{4.5}$$

$$DV_{CON} = V_{VP} - V_{inj} - \frac{V_{loop}}{2} \tag{4.6}$$

DV_{UV} is the dead volume between the injection loop and UV detector, V_{peak} is the volume at the peak in the absorbance profile, V_{inj} is the volume at which injection is performed, V_{loop} is the volume of the injection loop, DV_{CON} is the dead volume between the injection loop and conductivity cell and V_{VP} is the volume at the vertex point of the dip in the conductivity profile. The experiment was repeated two more times and a mean value was used in the modification of the experimental profiles.

The volume between the mixer and the injection loop, see figure 2, was not considered as dead volume but instead as wash volume. Since the volume between the mixer and the injection loop was easy to access it was physically measured.

4.4 Void fraction and total porosity

Void fraction and total porosity of the column were calculated with tracer experiments, similar to the dead volume experiment but with the column connected [2]. For the void fraction experiment a blue dextran solution was used [9]. Blue dextran is a large component that does not penetrate the porous structure of the particles. Since blue dextran absorb UV light a peak will appear in the absorbance profile, see figure 6. As seen in figure 6 the profile does not appear to be Gaussian, therefore the volume at the peak cannot be used directly when calculating the

void fraction. Instead the retention volume of the blue dextran was calculated as the first momentum, see equation (4.7) [2].

$$\mu_V = \frac{\int_0^\infty (V A_\lambda(V)) dV}{\int_0^\infty A_\lambda(V) dV} \tag{4.7}$$

The void fraction was calculated with equation (4.8).

$$\varepsilon_c = \frac{\mu_V - V_{inj} - DV_{UV} - \frac{V_{loop}}{2}}{V_c} \tag{4.8}$$

V_c is the total volume of the column.

For the total porosity experiment an acetone solution was used [10]. Acetone is a very small component that can penetrate the porous structure of the particles. Since acetone absorb UV light a peak will appear in the absorbance profile, see figure 7. The profile have a Gaussian appearance, therefore the volume at the peak can directly be used in the calculation of the total porosity, see equation (4.9).

$$\varepsilon = \frac{V_{peak} - V_{inj} - DV_{UV} - \frac{V_{loop}}{2}}{V_c} \tag{4.9}$$

4.5 Gradient elution at low multi-component column load

The parameters k_{kin}, B and β in the Langmuir MPM model, k_{des}, K_{eq} and v in the SMA model, k_{des}, K_{eq1} and v in the SAS model and k_f, H and β in GL model were calibrated using multi-component gradient elution experiments. A small amount of the protein mixture was loaded onto the column. To elute the proteins a linear salt gradient was applied. The experiments were performed using different salt gradients. The retention volumes and the shape of the experimental profiles, at different salt gradients, were used to calibrate the parameters [1]. Parameters in table 1 were adjusted in order to fit the simulated retention volumes of the different proteins and the shape of the simulated profiles to the experimental ones.

Table 1. Parameters that were calibrated using the retention volumes and the shape of the experimental profiles in the multi-component gradient elution experiments.

	Langmuir MPM model	SMA model	SAS model	GL model
Retention volumes	B	K_{eq}	K_{eq1}	H
	β	v	v	β
Shape of profiles	k_{kin}	k_{des}	k_{des}	k_f

Calibration was performed in MATLAB using the curve-fitting function lsqcurvefit with trust-region-reflective algorithm. The lsqcurvfit function requires good guess values on the parameters to perform well. To provide the function with guess values the parameters were first adjusted manually.

4.6 Gradient elution at high single-component column load

To calibrate the capacity parameters seen in table 2 mass overloaded single-component gradient elution experiments were performed. A sample with a high protein concentration was loaded onto the column. To elute the proteins a linear salt gradient was applied. Parameters in table 2 were adjusted in order to fit the simulated profiles to the experimental ones. The calibration was performed manually since it was difficult to get the experimental profiles and the simulated profiles to coincide, see figures 10, 11 and 12.

Table 2. The capacity parameters and the equilibrium constant that were calibrated using the shape of the experimental profiles in the single-component gradient elution experiments.

Langmuir MPM model	SMA model	SAS model	GL model
q_{max}	σ	σ	q_{max}
		K_{eq2}	

Since the Langmuir MPM model and SMA model could not capture the behavior of the mass overloaded experiments, see figures 10, 11 and 12, the above mentioned method could not be used to calibrate the capacity parameters for these models. Instead the data file for the column [11] was used to estimate the capacity parameters. In the data file a q_{max} value of $120\ mg/ml$ for lysozyme is documented. This value was used to calculate q_{max} for the other proteins by scaling q_{max} with the molecular weight of the proteins, see equation (4.10).

$$q_{max,i} = q_{max,lysozyme}\left(\frac{MW_i}{MW_{lysozyme}}\right) \tag{4.10}$$

MW_i is the molecular weight of protein *i*. In the data file a λ value of ca $0{,}12\ mmol/ml$ for the stationary phase is documented. This value was used to calculate the σ parameter for the different proteins, see equation (4.11).

$$\sigma_i = \frac{\Lambda}{q_{\mathrm{max,i}}} - v_i \tag{4.11}$$

4.7 Dispersion coefficient

For the Langmuir MPM model the dispersion coefficient was estimated with an empirical correlation [3], see equation (4.12).

$$Pe = \frac{v_{lin} d_p}{D_{ax}} \tag{4.12}$$

Pe is the Peclet number, v_{lin} is the linear velocity in the column and d_P is the particle diameter of the stationary phase. In the estimation of the dispersion coefficient the Peclet number was set to 0.5 [3].

For the other models the dispersion coefficient was calibrated the same way as the parameters in table 1, the dispersion coefficient was adjusted in order to fit the shape of the experimental profiles. By both adjusting the dispersion coefficient and the parameters in table 1 a better agreement between the simulated profiles and the experimental profiles was achieved.

4.8 Simulation technique

To solve the column model, partial differential equations (PDEs) were transformed to ordinary differential equations (ODEs). The space dimension was discretized into a number of grid points using the finite difference method [12]. This will generate an ODE for every grid point. The second order derivative in the PDEs was approximated with a 3-point central approximation as seen in equation (4.13) and the first order derivative in the PDEs was approximated with a 2-point backward approximation as seen in equation (4.14) [12].

$$\frac{\partial^2 c}{\partial x^2} = \frac{c_{n+1} - 2c_n + c_{n-1}}{h^2} \tag{4.13}$$

$$\frac{\partial c}{\partial x} = \frac{c_n - c_{n-1}}{h} \tag{4.14}$$

h is the distance between the grid points, and c_n is the concentration at grid point *n*. The number of grid points used was set to 100 since smaller discretization did not provide any noticeable changes in the solution. The generated ODEs were solved in MATLAB using an ODE solver (ode15s).

4.9 Optimization

To perform optimization different objects have to be considered. These objects are described in this section.

The optimization problem was solved in MATLAB using the nonlinear optimization function fmincon. During optimization the calibrated Langmuir MPM model was used.

4.9.1 Decision variables

Decision variables are the variables that are changed throughout the optimization to maximize or minimize the objective function. To keep the optimization problem simple and to simplify the interpretation of the optimization result, decision variables were limited to two variables. These variables are the loading volume and the final salt concentration in the linear salt gradient. The variables affect the purity and productivity obtained in a chromatographic run.

The lower and upper boundaries of the decision variables were chosen arbitrarily and can be seen in table 3.

Table 3. Lower and upper boundaries of the decision variables.

Decision variable	Lower boundary	Upper boundary
Loading volume	$0.1\ CV$	$12\ CV$
Final salt concentration	$250\ mM$	$500\ mM$

4.9.2 Design parameters

Design parameters are parameters that are constant during the optimization process. The design parameters that were used in the optimization process can be seen in table 4. Most parameters were similar to ones that were used in the experiments.

Table 4. Design parameters that were used in the optimization process.

Design parameter	Value
F	$0.5\ ml/min$
GL	$100\ CV$
$c_{lysozyme,Load}$	$2.5\ mg/ml$
$c_{Cytochrome\ C,Load}$	$2.5\ mg/ml$
$c_{Ribonuclease\ A,Load}$	$5.0\ mg/ml$
$c_{s,Load}$	$16{,}1\ mM$
$c_{s,start\ gradient}$	$200\ mM$

GL is the gradient length, $c_{i,Load}$ is the feed concentration of component *i* in the loading step, $c_{s,Load}$ is the salt concentration in the loading step and $c_{s,start\ gradient}$ is the start concentration of salt in the linear salt gradient.

4.9.3 Objective functions

Two common objective functions in chromatography are productivity and yield. For a chromatography system where the product is very expensive yield may be a more suitable objective function, whereas for a system where the product is less expensive productivity may be more suitable. In this optimization process an objective function that weighs both the productivity and yield, the normalized earning (NE) objective function [3], was used. Optimization was performed for different weighting factors. The objective functions are defined in equations (4.15), (4.16) and (4.17) [3].

$$Pr_i = \frac{c_{i,Load} V_{Load} Y_i}{t_c V_{sp}} \tag{4.15}$$

$$Y_i = \frac{\int_{t_1}^{t_2} c_i(t)\, dt}{c_{i,Load} t_{load}} \tag{4.16}$$

$$NE_i = w \frac{Pr_i}{\max(Pr_i)} + (1 - w) \frac{Y_i}{\max(Y_i)} \tag{4.17}$$

Pr_i is the productivity of component *i*, V_{Load} is the loading volume, Y_i is the yield of component *i*, t_c is the cycle time of the chromatography run, V_{sp} is the volume of stationary phase used in the column, t_{load} is the loading time, t_1 and t_2 are the cut times used when pooling component *i* and *w* is weighting factor. $\max(Pr_i)$ and $\max(Y_i)$ are obtained by optimizing equations (4.15) and (4.16) individually. In the optimization t_c was assumed to be equal to t_2, i.e. washing and regeneration time was not included.

During every simulation in the optimization a pooling decision have to be made. In this optimization process a completed function (simplexpooling), developed at the Department of Chemical engineering in Lund University, that optimizes the pooling with regard to the objective functions (4.15), (4.16) and (4.17) was used.

Cytochrome C was the second protein to elute in the chromatography process, therefore optimization was performed for the cytochrome C protein.

4.9.4 Constraints

Constraints define the valid space within the boundaries of the decision variables for an optimization process. They can be due to physical limitations or quality requirements. In this optimization process a minimum purity constraint of 99% was set for cytochrome C. The constraint was set in the pooling function. The purity of the different proteins was calculated using equation (4.18).

$$P_i = \frac{\int_{t_1}^{t_2} c_i(t)\, dt}{\sum_{J=1}^{N} \int_{t_1}^{t_2} c_j(t)\, dt} \tag{4.18}$$

5 Materials and experiments

5.1 Materials

Proteins that were used in the experiments are lysozyme from chicken egg white, cytochrome C from equine heart and ribonuclease A from bovine pancreas and were all obtained from Sigma-Aldrich. The properties of the three proteins can be seen in table 5 [13,14,15]. Protein mixtures were prepared by dissolving the proteins in a $20\,mM\ NaH_2PO_4$ buffer solution ($4.8\,pH$).

Table 5. Properties of the proteins used in the experiments.

Protein	MW (kDa)	pI (isoelectric point)
Lysozyme	14.307	11.35
Cytochrome C	12.384	$10.0 - 10.5$
Ribonuclease A	13.7	9.6

The column that was used in the experiments was a $1\,ml$ pre-packed column with a strong cation exchanger (Capto S), and was obtained from GE Healthcare Life Sciences. The stationary phase has an average particle diameter of $90\mu m$. Experiments were performed on a ÄKTA explorer chromatography system, from GE Healthcare Life Sciences, with an injection loop of $0.1\,ml$.

Buffer solutions were prepared by dissolving salt in deionized water. All the solutions were deaerated, using a vacuum pump, before usage to avoid introducing air into the column.

5.2 Experiments

All experiments were performed at ca 28℃ and all buffer solutions had a pH at ca 4.8. The flow rate was set to $0.5\,ml/min$ if nothing else is stated.

5.2.1 Experiments to determine the UV absorption coefficients

The feed concentration of lysozyme and cytochrome C was $2\,mg/ml$ and the feed concentration of ribonuclease A was $4\,mg/ml$. A gradient length of 5 column volumes (CV) was applied. The buffer solution was a $20\,mM\ NaH_2PO_4$ solution and the elution buffer was a $20\,mM\ NaH_2PO_4$ solution with $750\,mM\ NaCl$. The flow rate was set to $1\,ml/min$. After each experiment regeneration was performed for 12 CV.

5.2.2 Experiments to determine the dead volume and total porosity

A $275\,mM$ acetone solution was prepared in deionized water and used in the experiments. The mobile phase was a $20\,mM\ NaH_2PO_4$ buffer solution.

5.2.3 Experiment to determine void fraction

A $0.1\,mg/ml$ blue dextran solution was prepared in deionized water and used in the experiment. The mobile phase was a $20\,mM\ NaH_2PO_4$ buffer solution.

5.2.4 Gradient elution experiments at low multi-component column load

The feed concentration of lysozyme and cytochrome C was $2.5\ mg/ml$ and the feed concentration of ribonuclease A was $5\ mg/ml$. The buffer solution was a $20\ mM\ NaH_2PO_4$ solution with $100\ mM\ NaCl$ and the elution buffer was a $20\ mM\ NaH_2PO_4$ solution with $500\ mM\ NaCl$. Experiments were performed for five different gradient length of 25, 35, 45, 55 and 65 CV. After each experiment regeneration was performed for 12 CV.

Judging by the isoelectric point of the proteins in table 5 ribonuclease will elute first and lysozyme last. This was confirmed in [16], however a different but similar stationary phase was used.

5.2.5 Gradient elution experiments at high single-component column load

Five experiments were performed for lysozyme at the feed concentrations 12.5, 25, 50, 100 and $140\ mg/ml$. For cytochrome C and ribonuclease A only one experiment for each protein was performed at the feed concentration $50\ mg/ml$. The buffer solution was a $20\ mM\ NaH_2PO_4$ solution and the elution buffer was a $20\ mM\ NaH_2PO_4$ solution with $750\ mM\ NaCl$. A gradient length of 25 column volumes (CV) was applied. After each experiment regeneration was performed for 12 CV.

Cytochrome C and ribonuclease A are very expensive proteins. During this thesis only a small amount was provided, therefore the amount of experiments that could be performed were limited. Lysozyme on the other hand was less expensive and was provided at larger quantities, therefore several experiments were performed for lysozyme.

5.2.6 Validation experiment

Validation experiment was performed at moderate protein concentrations. The feed concentration of the protein mixture was $10\ mg/ml$ for each protein. The buffer solution was a $20\ mM\ NaH_2PO_4$ solution and the elution buffer was a $20\ mM\ NaH_2PO_4$ solution with $750\ mM\ NaCl$. A gradient length of 50 column volumes (CV) was applied.

A second validation experiment at higher column load would have been performed if not for the limitation of the available proteins.

6 Results

6.1 Model calibration

6.1.1 UV Absorption coefficients

The absorbance profiles obtained from the single-component experiments to determine the absorption coefficients of the different proteins can be seen in figure 3.

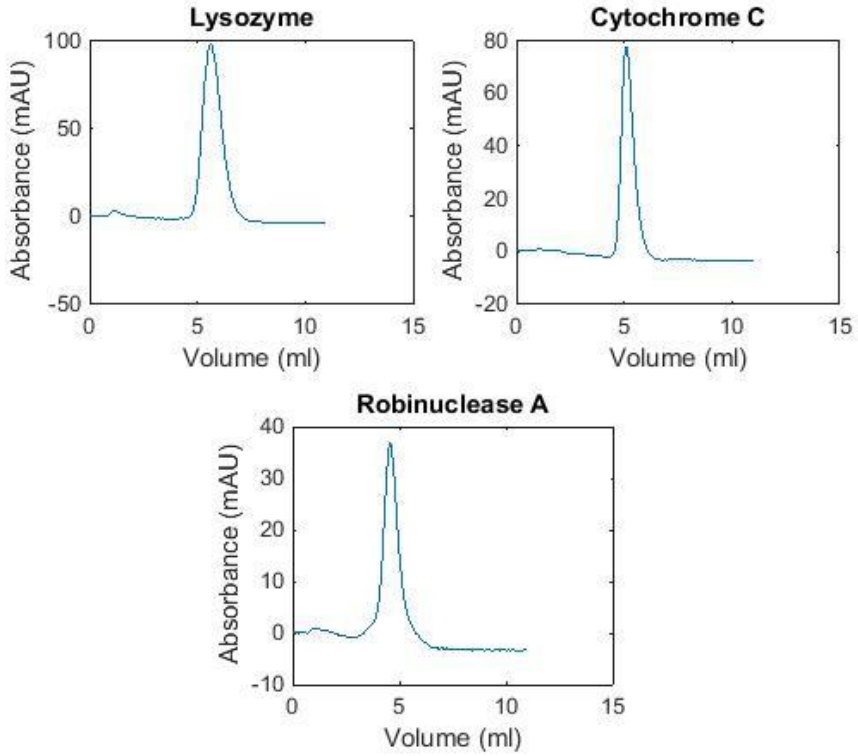

Figure 3. Absorbance profiles obtained from single-component experiments to determine the absorption coefficients of the different proteins at a wavelength of 280 nm.

The calculated absorption coefficients of the different proteins can be seen in table 6.

Table 6. Calculated absorption coefficients of the different proteins at a wavelength of 280 nm.

Protein	Absorption coefficient $((mAU \cdot ml)/mg)$
Lysozyme	516.69
Cytochrome C	305.47
Ribonuclease A	86.542

6.1.2 Conductivity

The proportionality constant was calculated by measuring the conductivity of a $500\ mM\ NaCl$ buffer solution, see equation (6.1).

$$A_{Con} = \frac{0.5\ mol/l}{40.65\ mS/cm} = 0.0123\ (mol \cdot cm)/(l \cdot mS) \quad (6.1)$$

6.1.3 Dead Volume

The absorbance and conductivity profiles obtained from the three tracer experiments to determine the dead volume can be seen in figures 4 and 5.

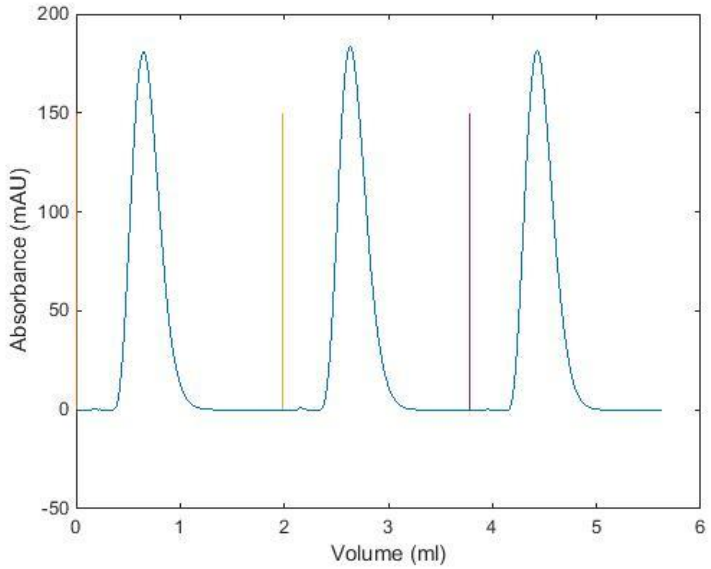

Figure 4. Absorbance profiles obtained from the three tracer experiments to determine the dead volume between the injection loop and UV detector.

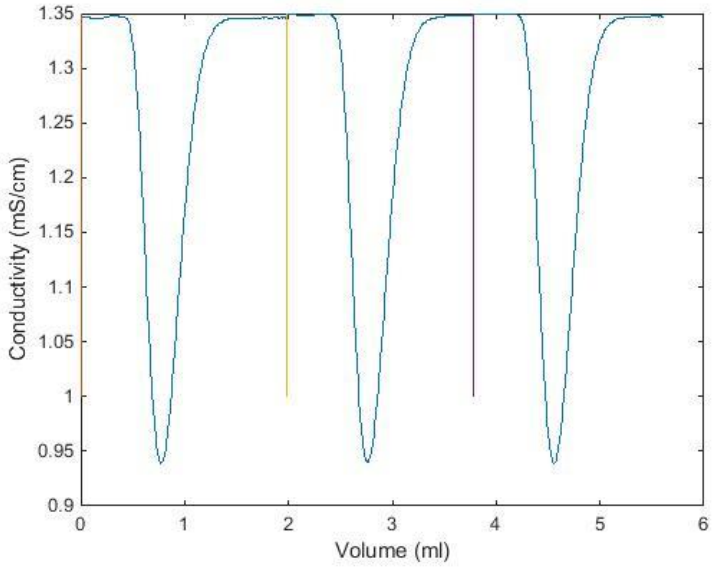

Figure 5. Conductivity profiles obtained from the three tracer experiments to determine the dead volume between the injection loop and conductivity cell.

The vertical lines in figures 4 and 5 indicates the volumes at which the injections of the acetone solution were performed. The dead volume between the injection loop and UV detector was calculated to $DV_{UV} = 0.6003\, ml$ and the dead volume between the injection loop and conductivity cell was calculated to $DV_{Con} = 0.7235\, ml$.

The wash volume between the mixer and injection loop, see figure 2, was measured to $0.266\, ml$.

6.1.4 Void fraction of the column and total porosity

The absorbance profile obtained from a tracer experiment to determine the void fraction of the column can be seen in figure 6.

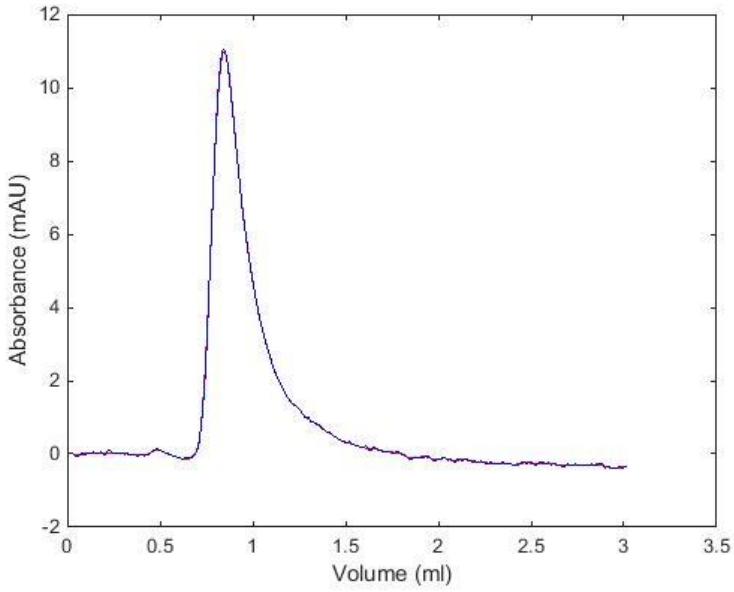

Figure 6. Absorbance profile obtained from a tracer experiment to determine the void fraction of the column.

Blue dextran solution was injected at volume $0\ ml$. The void fraction was calculated to $\varepsilon_c = 0.3123$.

The absorbance profiles obtained from the three tracer experiments to determine the total porosity of the column can be seen in figure 7.

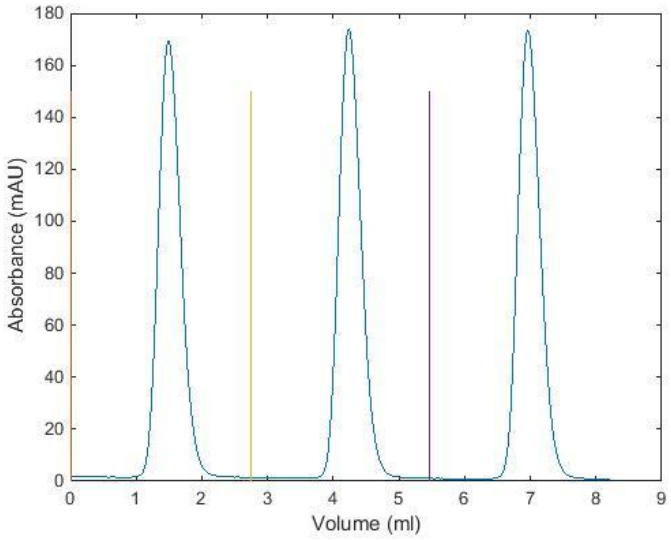

Figure 7. Absorbance profiles obtained from three tracer experiments to determine the total porosity of the column.

The total porosity of the column was calculated to $\varepsilon = 0.8468$.

6.1.5 Results from gradient elution experiments at low multi-component column load

Calibrated models fit to the multi-component calibration experiment with 25 CV gradient length can be seen in figures 8 and 9. The calibrated model parameters are listed in table 7.

Table 7. Calibrated model parameters from multi-component experiments at low column load.

Langmuir MPM model	Lysozyme	Cytochrome C	Ribonuclease A
$B\ [-]$	$10^{16.9781}$	$10^{15.8119}$	$10^{14.7077}$
$\beta\ [-]$	6.1698	5.8759	5.6446
$k_{kin}\ [s^{-1}]$	$10^{-1.6329}$	$10^{-1.2702}$	$10^{-1.7855}$
$D_{ax}\ [m^2/s]$	$10^{-7.3370}$	$10^{-7.3370}$	$10^{-7.3370}$
SMA model	Lysozyme	Cytochrome C	Ribonuclease A
$K_{eq}\ [-]$	$10^{4.0671}$	$10^{3.6091}$	$10^{3.0252}$
$v\ [-]$	5.8985	5.8242	5.5976
$k_{des}\ [m^3/(mol\ s)]$	$10^{-6.2936}$	$10^{-5.8701}$	$10^{-5.5355}$
$D_{ax}\ [m^2/s]$	$10^{-6.7370}$	$10^{-7.0370}$	$10^{-6.5370}$
SAS model	Lysozyme	Cytochrome C	Ribonuclease A
$K_{eq,1}\ [-]$	$10^{4.180}$	$10^{3.6351}$	$10^{3.0550}$
$v\ [-]$	6.1699	5.9942	5.8076
$k_{des}\ [m^3/(mol\ s)]$	$10^{-6.2447}$	$10^{-5.8701}$	$10^{-5.5355}$
$D_{ax}\ [m^2/s]$	$10^{-6.7370}$	$10^{-7.0370}$	$10^{-6.5370}$
GL model	Lysozyme	Cytochrome C	Ribonuclease A
$H\ [m^3/mol]$	$10^{17.0197}$	$10^{15.8234}$	$10^{14.7555}$
$\beta\ [-]$	6.1698	5.8759	5.6446
$k_f\ [s^{-1}]$	$10^{-0.2329}$	$10^{-0.0502}$	$10^{-0.585}$
$D_{ax}\ [m^2/s]$	$10^{-6.5588}$	$10^{-6.8600}$	$10^{-6.4919}$

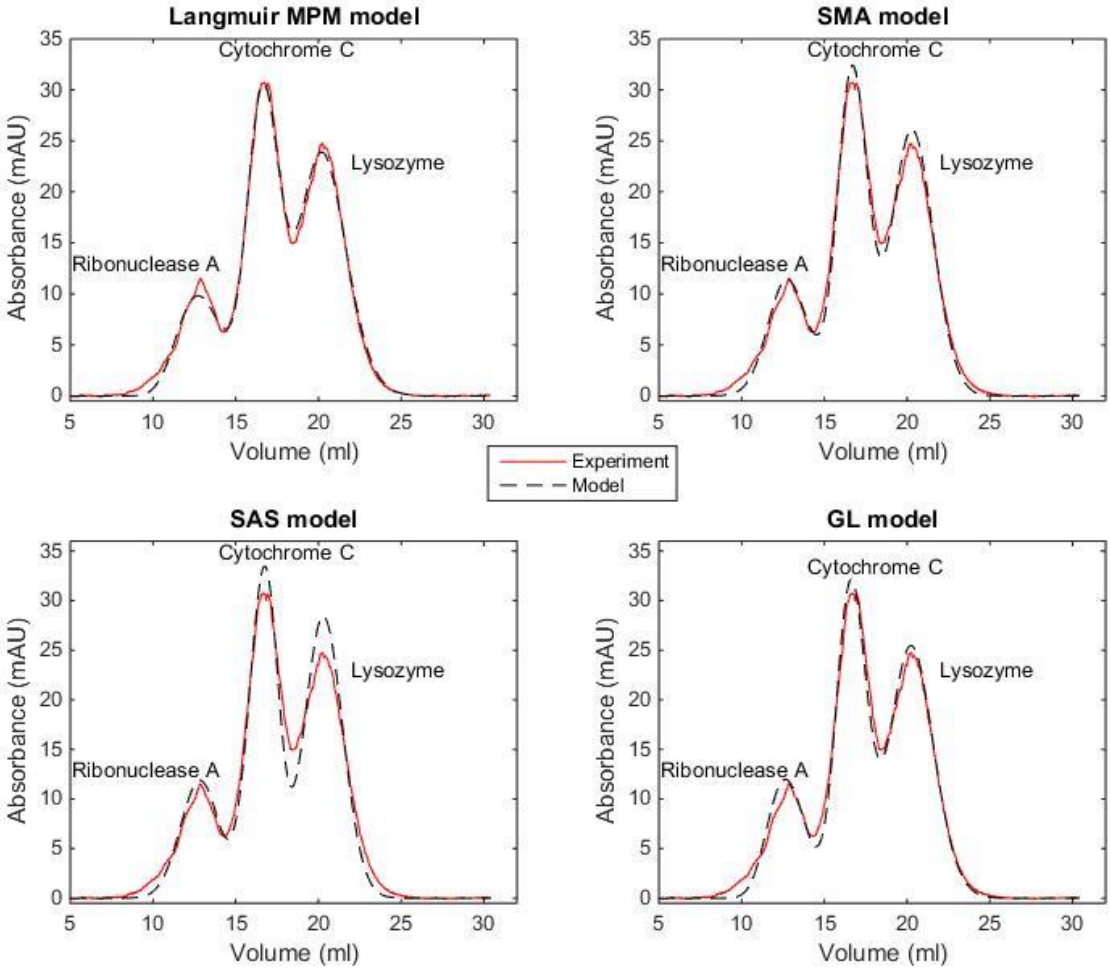

Figure 8. Calibrated models fit to the multi-component calibration experiment with $25\ CV$ *gradient length.*

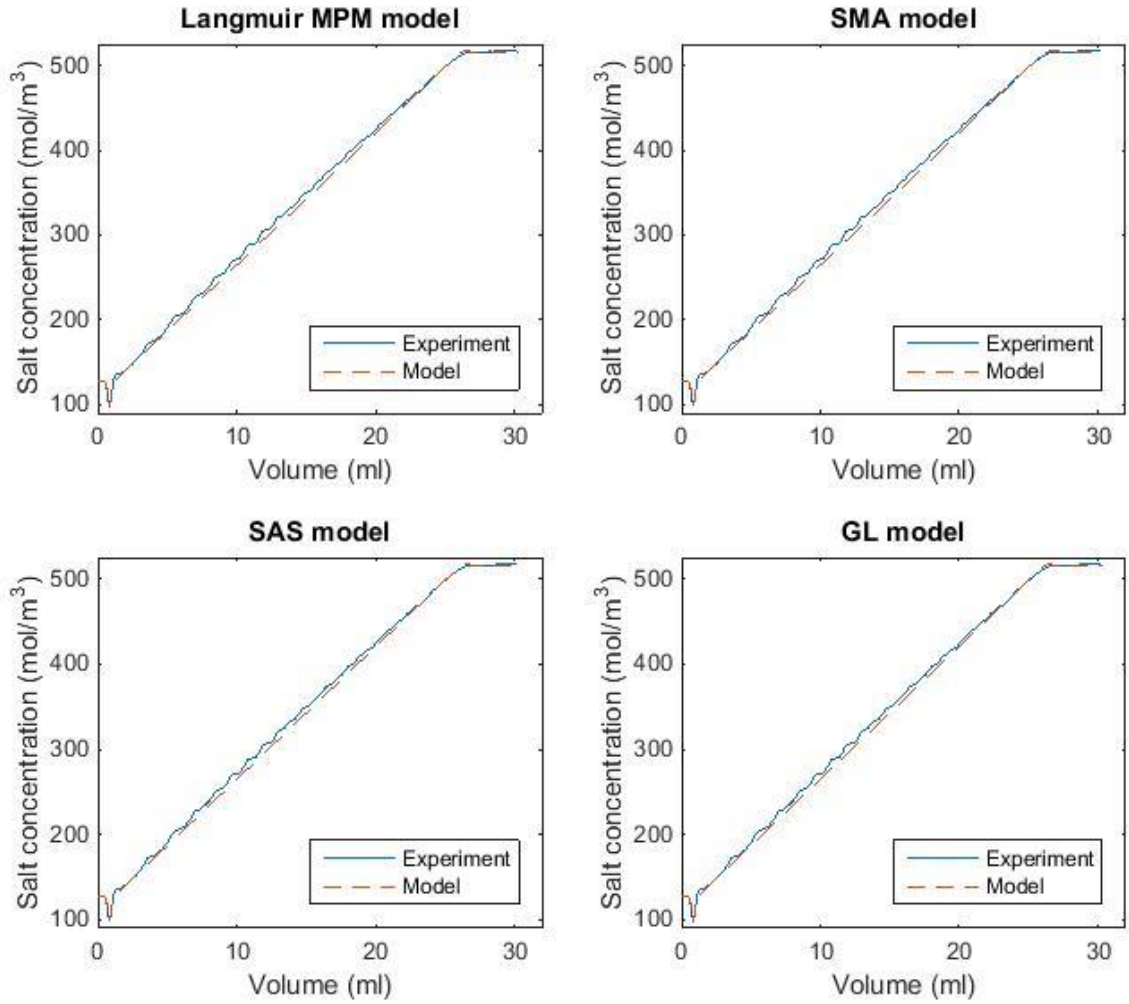

Figure 9. Corresponding salt concentration profiles to the multi-component calibration experiment with 25 *CV gradient length.*

In the SMA and SAS models a different concentration unit was used than in the Langmuir MPM and GL models. The unit $100\,mol/m^3$ was used instead of mol/m^3. This was done to minimize numerical errors in the simulation. When the unit mol/m^3 was used in the SMA and SAS models very small values were obtained for the calibrated k_{des} parameters. The values obtained were in the range of 10^{-20} i.e. values close to zero. By scaling the concentration unit larger values for the calibrated k_{des} parameters were obtained, see table 7.

6.1.6 Results from gradient elution experiments at high single-component column load

Calibrated models fit to the mass overloaded calibration experiments can be seen in figures 10, 11 and 12. The calibrated model parameters are listed in table 8.

Table 8. Calibrated model parameters from single-component experiments at high column load.

Langmuir MPM model	Lysozyme	Cytochrome C	Ribonuclease A
q_{max} $[mol/m^3]$	8.3875	11.1946	9.1472
SMA model	Lysozyme	Cytochrome C	Ribonuclease A
σ $[-]$	8.4085	4.8953	7.5212
SAS model	Lysozyme	Cytochrome C	Ribonuclease A
$K_{eq,2}$ $[-]$	$10^{2.65}$	$10^{3.00}$	$10^{3.0}$
σ $[-]$	-3.0000	-1.0000	2.000
GL model	Lysozyme	Cytochrome C	Ribonuclease A
q_{max} $[m^3/mol]$	8.3875	6.7168	3.6589

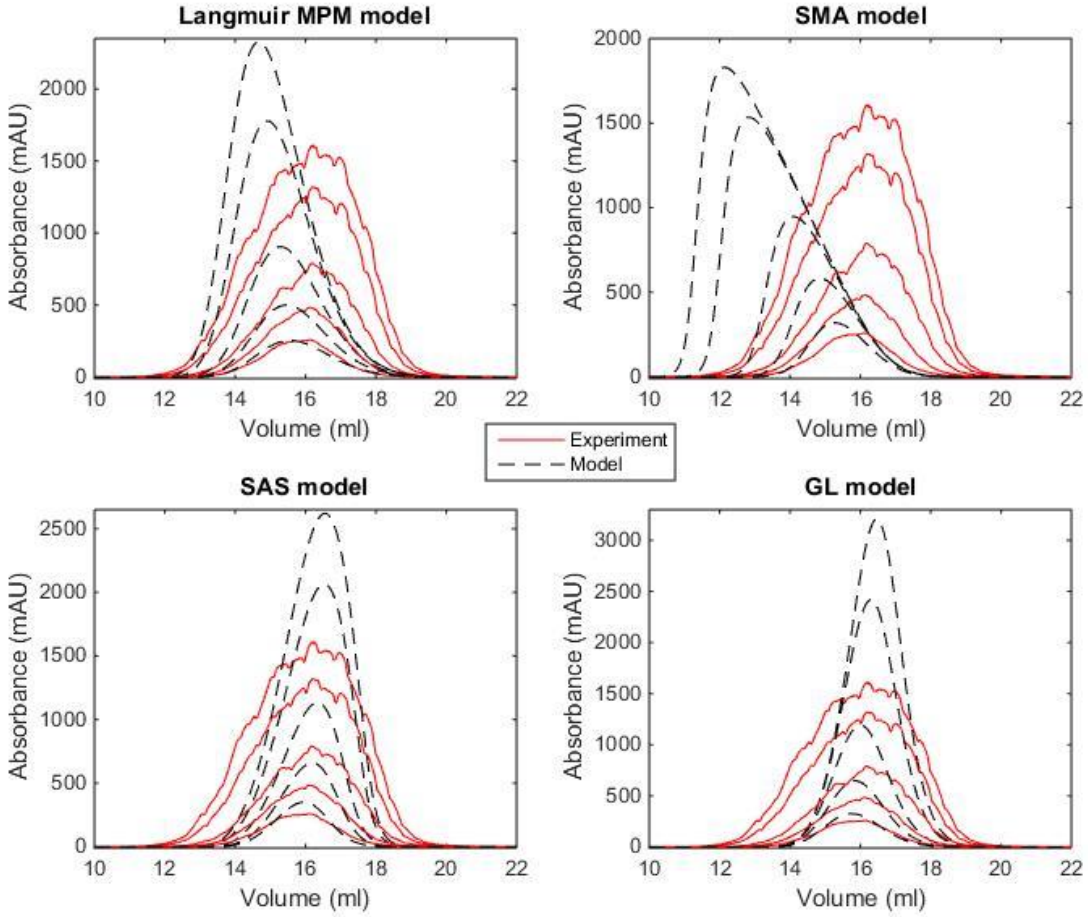

Figure 10. Calibrated models fit to single-component experiments at different lysozyme feed concentrations (12.5, 25, 50, 100 and 140 mg/ml).

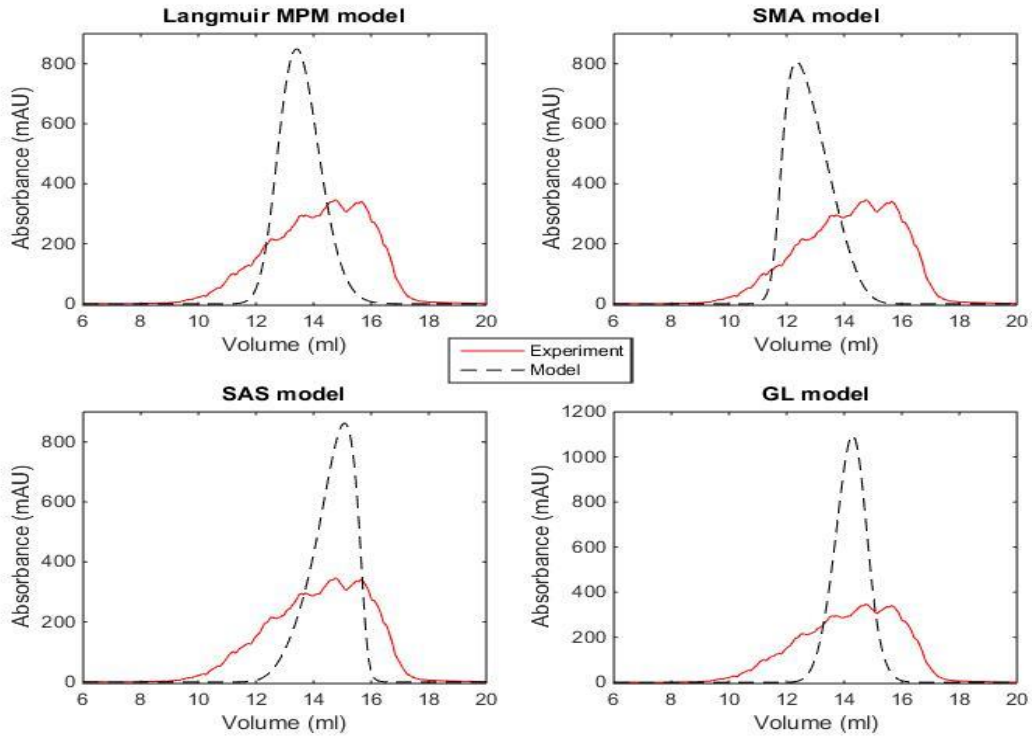

Figure 11. Calibrated models fit to single-component experiment at 50 mg/ml cytochrome C feed concentration.

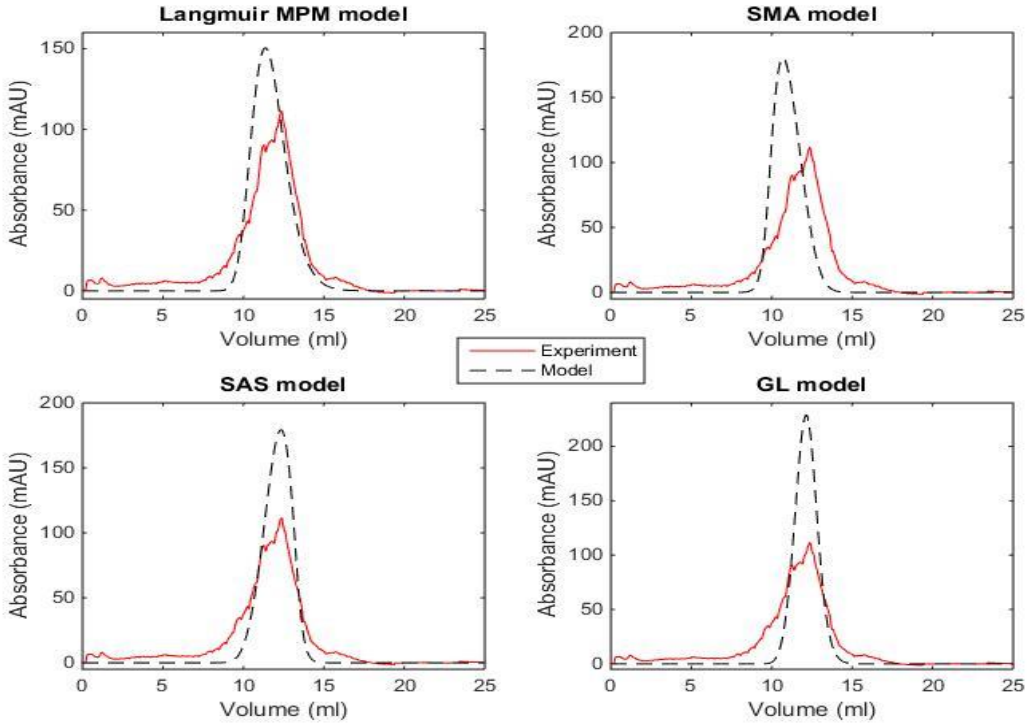

Figure 12. Calibrated models fit to single-component experiment at 50 mg/ml ribonuclease A feed concentration.

Salt concentration profiles were not presented since they fit very well to the experimental profiles and are similar to the profiles in figure 9.

6.1.7 Results from validation experiment

The result from the validation experiment can be seen in figure 13.

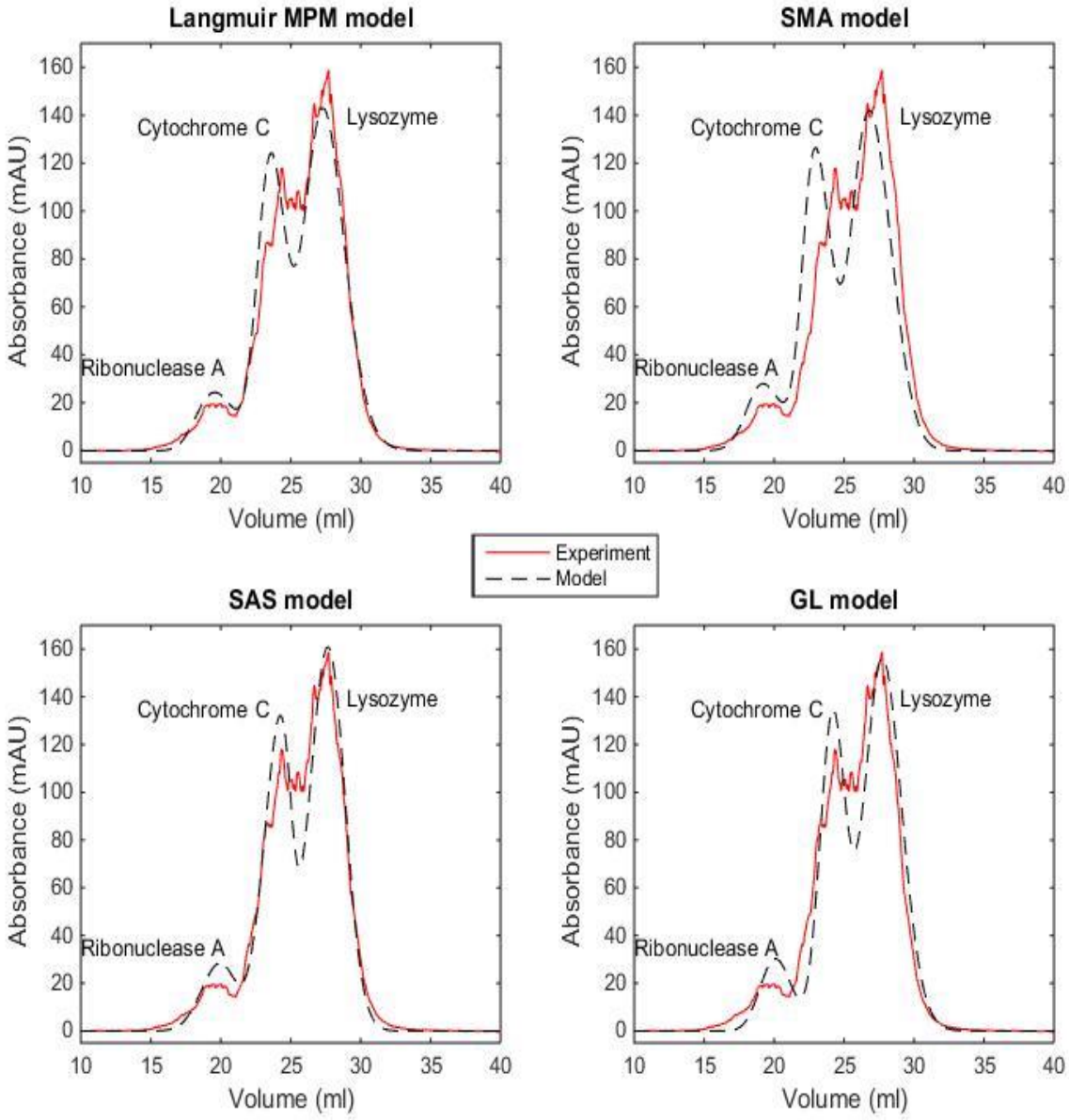

Figure 13. The validation experiment for the different models.

6.2 Optimization

Maximum productivity and yield obtained at their respective operating conditions can be seen in table 9.

Table 9. Operating conditions at maximum productivity and yield.

Objective function	Max objective function value	Loading volume (ml)	Final salt concentration (mM)
Productivity	$4.725\ g/(s \cdot m^3)$	9.390	500.0
Yield	99.90%	0.5126	267.68

Optimization was performed for the NE objective function at weighting factors ranging from 0.05 to 0.95. Productivity and yield obtained at the different weighting factors can be seen in figure 14. The operating conditions at the different weighting factors can be seen in figure 15.

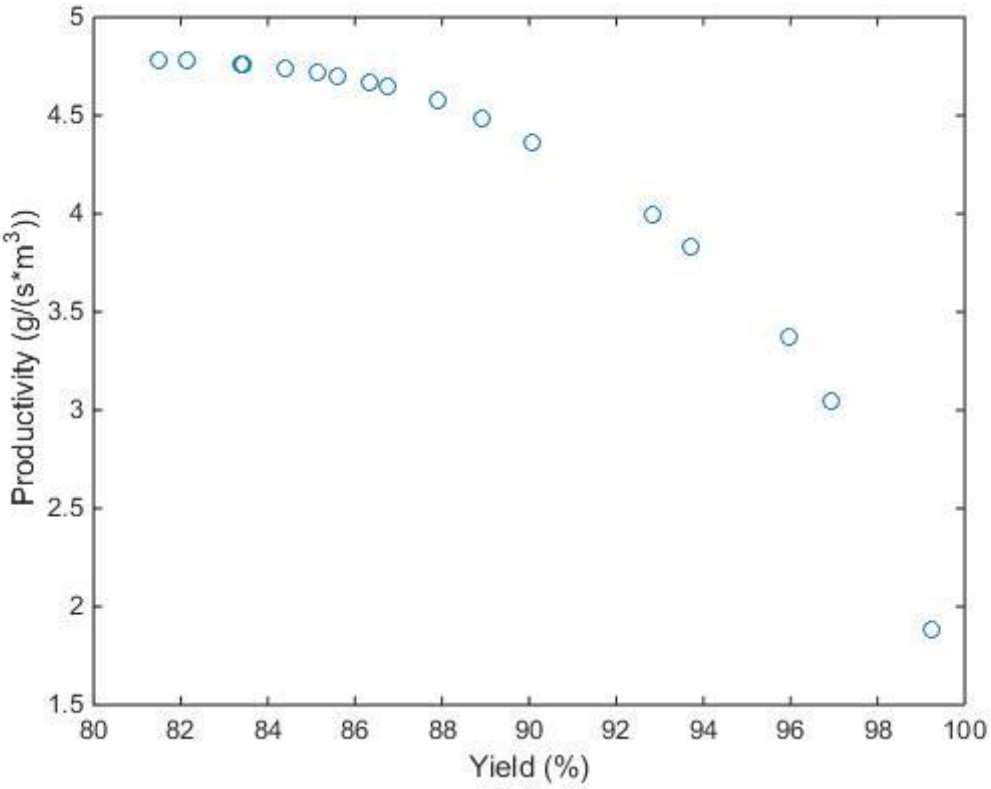

Figure 14. Productivity and yield obtained at different weighting factors when optimizing the NE objective function.

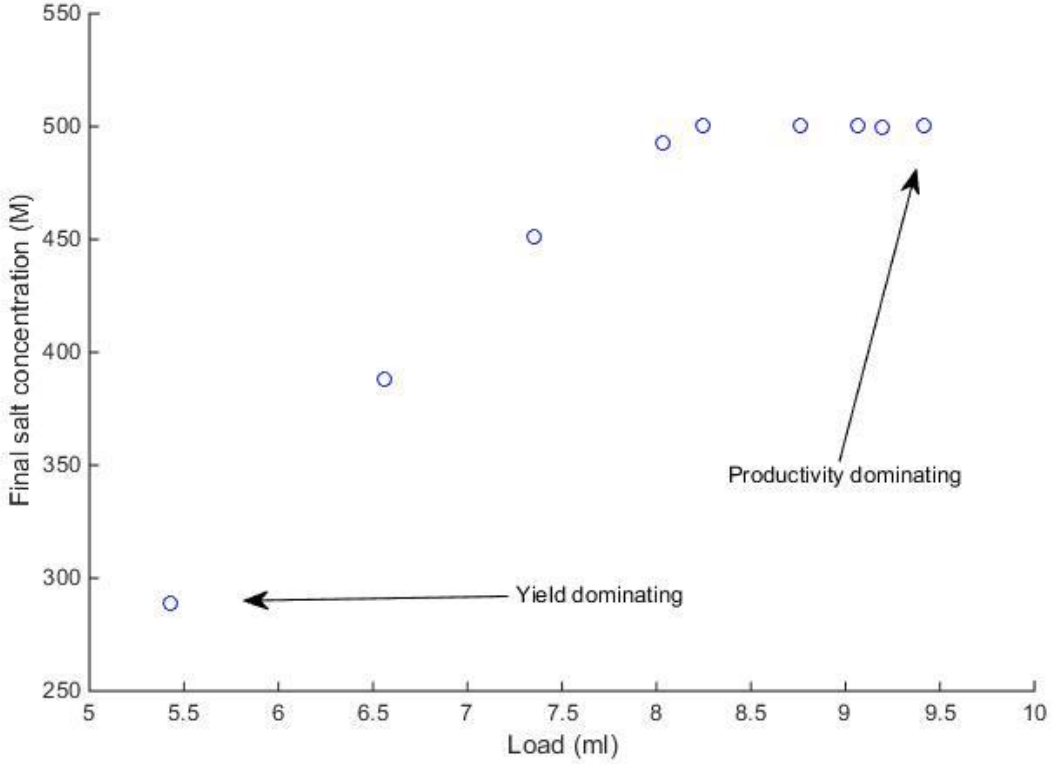

Figure 15. Optimal operating conditions at different weighting factors for the NE objective function.

7 Discussion

7.1 Model calibration

7.1.1 Column model

When choosing a column model different factors have to be considered. A complex model that describes various phenomena can provide a better precision, higher flexibility and a better understanding of the system. But a complex model would also require more experiments to calibrate and longer computation times to simulate. Therefore it´s a matter of weighting the different factors and defining the limitations of the model, when choosing a column model.

In this thesis a column model of an intermediate complexity was chosen. The kinetic dispersive model is a model that lumps different phenomena together and expresses them as convection, dispersion and adsorption kinetics. The model is particularly suitable for modelling systems where the mass transfer in the stationary phase can be neglected [5]. This is the case for systems that consist of small proteins, as in this thesis, with high diffusivity and small stationary phase. The model requires few experiments to calibrate and has a short computational time when simulating. Therefore the kinetic dispersive model was considered suitable in this thesis.

7.1.2 Adsorption model

In the initial stage of this thesis a literature study was done. In several articles [9,17,18,19] the isotherm of the three proteins were experimentally verified. [18] shows that for a different but similar stationary phase the three proteins follow the Langmuir isotherm. [9] verifies that lysozyme follows the Langmuir isotherm when the same stationary phase (Capto S) is used. Based on this two adsorption models, the Langmuir MPM modal and the SMA model, were considered suitable since they express the behavior of a Langmuir isotherm.

When the mass overloaded experiments were performed a different behavior than expected was observed. All three proteins showed concentration profiles that do not agree with the Langmuir isotherm. When the experimental profiles in figures 10, 11 and 12 were compared to the profiles in figure 1, the proteins seemed at first to follow an anti-Langmuir isotherm. In an attempt to capture that behavior two additional adsorption models were calibrated, the SAS model and GL model. The result of the calibration of the SAS model and GL model to the mass overloaded experiments can be seen in figures 10, 11 and 12, even these models did not fit the experimental profiles very well. As mentioned in the theory section the SAS model has an anti-Langmuir behavior at low concentrations and Langmuir-behavior at high concentrations. To fit the SAS model to the experimental profiles in figures 10 and 11 extreme values had to be set on the σ parameter, see table 8. Negative values on σ has no actual physical meaning, but was necessary to calibrate the model.

When the experimental profiles in figure 10 were further analyzed a different conclusion was reached on the isotherm of the proteins. In figure 1 it can be seen that for an anti-Langmuir isotherm the concentration profiles tend to shift to the right when the feed concentration is increased, that is not the whole case for the experimental profiles in figure 10. The experimental profiles in figure 10 shift to the right a little bit at lower feed concentrations, but at higher feed concentrations the experimental profiles cease to move. It appears as if the proteins follow an

isotherm that has an anti-Langmuir behavior at lower concentrations and a linear behavior at higher concentrations.

It is very difficult to explain why the concentration profiles of the proteins did not agree with Langmuir isotherm, as the other articles suggested, and why they behaved as they did. One explanation may be the solubility of the proteins. In the articles [9,17,18,19] the experiments to verify the isotherm of the proteins are different from the experiments that were performed in this thesis. In the articles, batch experiments were performed to obtain the isotherm of the proteins. Batch experiments were performed by placing the stationary phase in a protein solution for some amount of time. The concentration of the protein solution was then measured and the concentration in the stationary phase was calculated. The concentrations of the protein solutions that were used in the batch experiments were very low compared the concentrations of the mass overloaded experiments. In the batch experiments the concentrations of the protein solutions did not exceed $5\,mg/ml$ whereas the concentrations in the mass overloaded experiments were between $12.5\,mg/ml$ and $140\,mg/ml$. The proteins might have poor solubility property so that at high protein concentrations two phases are formed, which then causes the behavior seen in figures 10, 11 and 12. Similar behavior to the experimental profiles in figures 10, 11 and 12 can be seen for a different system in [2]. The system stated in [2] is a reversed-phase chromatography system and has a mobile phase that consist of 60% methanol and 40% water. The mixture that is injected in the system is pure methanol. Due to the difference in the solubility of the component in the mobile phase and in the injected mixture, the peak of the component distort and the same behavior as in figures 10, 11 and 12 is seen.

By looking at the calibration experiments and the validation experiment it can be concluded that the models have a good agreement with the experiments only at low column loads. At higher column load only the SAS model and GL model capture the behavior of the experimental profiles to a certain degree. The models that were calibrated should only be used within the concentrations of the calibration experiments, unless a validation experiment is performed to ensure the validity of the models at other concentrations.

7.1.3 Column parameters

The void fraction of the column and the total porosity were calculated to $\varepsilon_c = 0.3123$ and $\varepsilon = 0.8468$. In [2] it is stated that for spherical and monodisperse adsorbents the void fraction usually lies in the range of $0.26 < \varepsilon_c < 0.48$ and the total porosity lies in the range of $0.65 < \varepsilon < 0.80$. Based on this the calculated ε is a little bit too high. The calculated column parameters were assumed to be valid and were therefor used in the modeling.

7.2 Optimization

Since other articles suggest that the proteins follow the Langmuir isotherm, the Langmuir MPM model was used during the optimization process, even though the model did not fit the experimental profiles very well at high column load.

The result from the optimization process is straightforward and easy to interpret since the optimization problem was kept simple by only having two decision variables and one purity constraint. The operating conditions obtained at maximum productivity and maximum yield can be seen in table 9. Maximum productivity is obtained at high loading volume and steep salt gradient. Steep salt gradient is applied to elute the proteins quicker and decrease the cycle time.

Maximum yield is obtained at low loading volume and flat salt gradient. Flat salt gradient allows the proteins to separate more efficiently, this will provide a higher yield when a purity constraint is present. More efficient separation of the proteins is also obtained at low column loads.

The NE objective function weighs both the productivity and yield. Figure 15 shows how the operating conditions change depending on the dominating factor in the NE objective function. In figure 15 it can be observed that several optimal operating conditions are located at the upper boundary of the salt concentration. This means that these optimal operating conditions are probably only local optimal operating conditions and that the global optimal operating conditions are probably located at higher salt concentration. Therefore a higher salt concentration than $500\ mM$ should be set as the upper boundary. To avoid extrapolation the upper boundary should not exceed a value of $750\ mM$.

7.3 Further work

The proteins that were studied in this thesis behaved differently than expected. A different behavior than the expected Langmuir isotherm was observed. One possible explanation was that the behavior is due to the poor solubility of the proteins. This can probably be verified by performing volume overloaded experiments. The experiment is performed by injecting a large volume of a mixture with low protein concentration. If the concentration profiles show Langmuir behavior then the suggested explanation is probably valid.

The capacity parameters in table 2 were calibrated by performing only one calibration experiment for cytochrome C and ribonuclease A. To perform a proper calibration several calibration experiments should be performed.

The result from the optimization shows that maximum productivity is obtained at high loading volumes. All the experiments were performed by injecting a volume of $0.1\ ml$. To ensure the validity of the model at high loading volumes both calibration experiments and validation experiments should be performed at high loading volumes.

8 Conclusion

The method that was used to calibrate the models was simple and only required few experiments. All the models, especially the Langmuir MPM, have a good agreement with the experiments at low column load. At higher column load only two models, SAS and GL, capture the behavior of the experiments to a certain degree.

When mass overloaded experiments were performed the proteins behaved different than expected. The concentration profiles of the mass overloaded experiments did not agree with Langmuir isotherm. Why the proteins behaved differently is unknown. One suggestion is that proteins have poor solubility. At high protein concentrations two phases are formed and that would cause the concentration profiles to distort.

The result from the optimization was expected and easy to interpret. Maximum productivity is obtained at high loading volume and steep salt gradient while maximum yield is obtained at low loading volume and flat salt gradient.

9 Nomenclature

Subscript i stands for the three proteins used in this thesis lysozyme, cytochrome C and ribonuclease A.

A	The cross-sectional area of the column $[m^2]$
A_{Con}	Proportionality constant between conductivity and salt concentration $[\frac{mol \cdot cm}{l \cdot mS}]$
A_λ	Absorbance at a specific wavelength λ $[mAU]$
Abs_λ	Absorption coefficient at a specific wavelength λ $[(mAU \cdot ml)/mg]$
B	Kinetic coefficient $[-]$
c	Concentration of the dissolved component $[mg/ml]$
c_i	Concentration in the mobile phase $[mol/m^3]$
$c_{i,Load}$	Feed concentration in the loading step $[mol/m^3]$
$c_{inlet,i}$	Inlet concentration of the mobile phase $[mol/m^3]$
c_n	Concentration at grid point *n* $[mol/m^3]$
c_s	Salt concentration in the mobile phase $[mol/m^3]$
$c_{s,Load}$	Salt concentration in the loading step $[mol/m^3]$
$c_{s,start\ gradient}$	Start concentration of salt in the linear salt gradient $[mol/m^3]$
$c_{s,wash}$	Salt concentration in the mobile phase that is used to wash the column $[mol/m^3]$
Con	Conductivity $[mS/cm]$
d_p	Particle diameter of the stationary phase $[m]$
D_{ax}	Axial dispersion coefficient $[m^2/s]$
DV_{CON}	Dead volume between the injection loop and conductivity cell $[ml]$
DV_{UV}	Dead volume between the injection loop and the UV detector $[ml]$
F	Volumetric flow $[m^3/s]$
GL	Gradient length [CV]

h	Length between grid points $[m]$
H_i	Henry's constant $[m^3/mol]$
$k_{ads,i}$	Adsorption coefficient $[m^3/(mol\ s)]$
$k_{des,i}$	Desorption coefficient $[m^3/(mol\ s)]$
$k_{des0,i}$	Modulator constant $[m^3/(mol\ s)]$
$k_{f,i}$	Kinetic coefficient $[s^{-1}]$
$k_{kin,i}$	Kinetic coefficient $[s^{-1}]$
K_i	Equilibrium constant of adsorption, GL model $[-]$
$K_{eq,i}$	Equilibrium constant of adsorption, SMA model $[-]$
$K_{eq1,i}$	Equilibrium constant of adsorption, SAS model $[-]$
$K_{eq2,i}$	Equilibrium constant of dimerization, SAS model $[-]$
l	Light path length $[cm]$
L	Column length $[m]$
MW_i	Molecular weight $[g/mol]$
p_i	Model parameter, GL model $[-]$
P_i	Purity $[-]$
P_e	Peclet number $[-]$
$\mathrm{Pr_i}$	Productivity $[g/(m^3 s)]$
q_i	Concentration in the stationary phase $[mol/m^3]$
$\bar{q_s}$	Concentration of available ligands, SMA/SAS models $[mol/m^3]$
$q_{free,i}$	Concentration of available ligands, Langmuir MPM model $[mol/m^3]$
$q_{max,i}$	Maximum concentration attainable in the stationary phase $[mol/m^3]$
t	Time $[s]$
t_1	The first cut time when performing pooling $[s]$
t_2	The second cut time when performing pooling $[s]$

t_c	Cycle time of the chromatography run $[s]$
t_{load}	Loading time $[s]$
v_{lin}	Linear velocity in the column $[m/s]$
V	Volume $[m^3]$
V_c	Column volume $[m^3]$
V_{inj}	The volume at which injection is performed $[m^3]$
V_{load}	Loading volume $[m^3]$
V_{loop}	Volume of the injection loop $[m^3]$
V_{peak}	Volume at the peak in the absorbance profile $[ml]$
V_{sp}	Volume of the stationary phase $[m^3]$
V_{VP}	Volume at the vertex point of the dip in the conductivity profile $[ml]$
w	Weighting factor $[-]$
x	Length coordinate along the column [m]
Y_i	Yield $[-]$
β_i	Constant parameter that describes the ion-exchange characteristic $[-]$
ε	Total porosity of the column $[-]$
ε_c	Void fraction of the column $[-]$
μ_V	Retention volume $[ml]$
ν_i	Number of ligands that a protein adsorb to $[-]$
Λ	Ligand density in the stationary phase $[mol/m^3]$
σ_i	Steric factor $[-]$

10 References

[1] N. Jakobsson, A Model-Based Approach to Robustness Analysis and Optimisation of Chromatography Process, Lund University, Sweden, Department of Chemical Engineering, 2006.

[2] Henner Schmidt-Traub, Preparative Chromatography, Wiley-VCH Verlag GmbH & Co. KGaA, Weinheim, 2005.

[3] D. Karlsson, N. Jakobsson, A. Axelsson, B. Nilsson, Model-based optimization of a preparative ion-exchange step for antibody purification, Journal of Chromatography A, 1055 (2004) 29-39.

[4] B. Nilsson, Process Simulation Course, Modelling and Simulation III – Space Dependent Systems Part B, Lund University, Sweden, Department of Chemical Engineering, 2014.

[5] K. Westerberg, Modeling for Quality and Safety in Biopharmaceutical Production Processes, Lund University, Sweden, Department of Chemical Engineering, 2012.

[6] Jorgen M. Mollerup, A Review of the Thermodynamics of Protein Association to Ligands, Protein Adsorption, and Adsorption Isotherms, Chem. Eng. Technol. 2008, 31, No. 6, 864-874.

[7] M. Mazzotti, Equilibrium theory based design of simulated moving bed processes for a generalized Langmuir isotherm, Journal of Chromatography A, 1126 (2006) 311-322.

[8] Pierce Biotechnology, Extinction Coefficients, A guide to understanding extinction coefficients, with emphasis on spectrophotometric determination of protein concentration, Technical Resource, 2002.

[9] B. D. Bowes, H. Koku, K. J. Czymmek and A. M. Lenhoff, Protein adsorption and transport in dextran-modified ion-exchange media I. Adsorption, Journal of chromatography A 2009 November 6; 1216(45): 7774-7784.

[10] A. Osberghaus, S. Hepbildikler, S. Nath, M. Haindl, E. von Lieres and J. Hubbuch, Determination of parameters for the steric mass action model-A comparison between two appreoaches, Journal of Chromatography A, 1233(2012) 54-65.

[11] GE Healthcare Life Sciences, Data file 11-0025-76 AG, IEX, GE Healthcare Bio-Sciences AB, Björkgatan 30, 751 84 Uppsala, Sweden, 2012.

[12] B. Nilsson, Process Simulation Course, Modelling and Simulation III – Space Dependent Systems Part A, Lund University, Sweden, Department of Chemical Engineering, 2014.

[13] Sigma-Aldrich, Data sheet, Product number L7651, 3050 Spruce Street, St Louis, MO 63103 USA.

[14] Sigma-Aldrich, Data sheet, Product number C2506, 3050 Spruce Street, St Louis, MO 63103 USA.

[15] Sigma-Aldrich, Data sheet, Product number R5503, 3050 Spruce Street, St Louis, MO 63103 USA.

[16] N. Brestrich, T. Briskot, A. Osberghaus, J. Hubbuch (2014), A tool for selective inline quantification of co-eluting proteins in chromatography using spectral analysis and partial least squares regression. Biotechnol. Bioeng., 111: 1365–1373

[17] C. Martin, G. Iberer, A. Ubiera, G. Carta, Two-component protein adsorption kinetics in porous ion exchange media, Journal of Chromatography, 1079 (2005) 105-115.

[18] X. Xu, A. M. Lenhoff, A Predictive Approach to Correlating Protein Adsorption Isotherms on Ion-Exchange Media, J. Phys. Chem. B 2008, 112, 1028-1040.

[19] C. Chang, A. M. Lenhoff, Comparison of protein adsorption isotherms and uptake rates in preparative cation-exchange materials, Journal of Chromatography A, 827 (1998) 281-293.